Seismic Performance Evaluation of Corroded Steel Bridge Bearings

X. Fan & J. McCormick
University of Michigan, Ann Arbor, MI, USA

15 WCEE
LISBOA 2012

SUMMARY:
Steel bridge bearings, including bolster and rocker bearings, have been commonly used for older highway bypass bridges because of their ability to accommodate thermal expansion and contraction through rounded contact surfaces as well as their low cost. However in seismic regions, these steel bearings can be a weak link because they traditionally have not been designed for seismic loads and are susceptible to age related deterioration due to corrosion over time. Considering the critical role steel bearings play in the overall seismic response of a bridge, this paper explores the effects of different vertical loads and friction coefficients, which can change due to the presence of corrosion, on the bearing behavior under cyclic loading through computational finite element modeling. Theoretical formulations for the behavior of both bolster (fixed) and rocker (expansion) steel bearings under longitudinal and transverse loads also are developed to confirm the findings.

Keywords: steel bridges, bridge bearings, corrosion, aging, seismic

1. INTRODUCTION

Prior to learning their susceptibility to poor performance under large earthquake loads, fixed and expansion type steel bearings were extensively used in steel bridges as a load transfer mechanism and a means of accommodating translation and rotation of the superstructure. A large variety of these steel bearings are still in use today in older steel girder bridge systems, particularly in areas of the United States that are susceptible to moderate and large earthquakes with longer return periods (Padgett and DesRoches 2008). These bearings rely on a variety of passive mechanisms to accommodate displacements and rotations induced by temperature changes and vehicular movement, but are not designed to accommodate the forces and displacements induced by a seismic event.

Steel bolster (fixed) and rocker (expansion) bearings are two types of common bearings found in the Central and Eastern United States. The bolster bearing has a cylindrical surface at the top of the bearing to allow for rotations, while the rocker bearing uses cylindrical surfaces at the top and bottom of the bearing to accommodate both longitudinal displacement and rotation. Both types of bearing have pintles, or small protrusions, to restrain transverse displacement of the superstructure relative to the bearing. Along with their susceptibility to earthquake loading, the steel bearings are also predisposed to the effects of corrosion requiring regular maintenance and repainting. Lack of proper maintenance can lead to corrosion and debris buildup seriously limiting the ability of the bearing to function properly. As a result, the combined effects of aging/corrosion and seismic load can lead to significant performance deterioration of the steel bearing and steel bridge system. This is particularly important in light of the fact that steel bridge bearings are readily identified as the most vulnerable component in common classes of multiple span steel bridges (Nielson and DesRoches 2007).

Age-related deterioration of bridges manifests itself in a variety of patterns, among which corrosion of steel components is of particular concern and can result in unpredictable behavior. Although recent trends have been toward the use of elastomeric bearings in new construction, a significant number of

steel bridges in earthquake susceptible areas still utilize steel bearings (Brinkerhoff 1993). Steel bearings are particularly susceptible to decreased capacity from exposure to sea water in coastal regions and deicing salts in snow prone regions which subject steel bridge components to corrosion inducing chlorides (Kayser and Nowak 1989). In the absence of regular maintenance, corrosion of steel bridge bearings often leads to geometry changes and debris build-up at the contact surfaces. This process can accumulate significant amounts of corrosion product over time leading to unpredictable performance and possible "frozen" or "locked" conditions (Brinkerhoff 1993). The 2008 failure of the Birmingham Bridge in Pittsburgh was largely attributed to accelerated corrosion and debris buildup in the rocker bearing system. The corrosion and debris build-up restrained the mobility of the rocker bearing and induced excessive unidirectional rotation that caused the rocker bearing system to be unstable (Splitstone et al. 2010). Also, post-earthquake reconnaissance has revealed the potential role that corrosion may play in bridge bearing failures (Unjoh et al. 2008). However, few studies have attempted to characterize the behavior of corroded bridge bearings either numerically or through experimental testing.

Past analytical studies have shown the role that bridge bearings play in influencing the response of bridge systems under seismic loads. Bearing rotational stiffness (Dicleli and Bruneau 1995), variation in the coefficient of friction associated with expansion bearings (Pan et al. 2010), and bearing failures (Shinozuka et al 2000) have all been explored, but these parameters have not been correlated with aging effects. Experimental studies by Mander et al. (1996) and Barker and Hartnagel (1998) are the only two studies to focus on the cyclic response of steel rocker and bolster bearings to examine their expected hysteretic behavior under seismic loads. Quasi-rectangular hysteresis loops for the steel rocker bearings and elliptical hysteresis loops for the steel bolster bearings were observed and it was found that Coulomb friction governed the rigid sliding behavior observed in the response of the bearings. However, correlation between hysteretic behavior and parameters affected by corrosion level (such as friction coefficient) was not explicitly considered. In light of these past findings, there still exists a need to develop models that can be used to evaluate steel bearings under cyclic loads and investigate the effects of corrosion and other parameters on their performance.

This paper addresses this need through an extensive finite element study. A theoretical analysis of the expected behavior and failure mechanism of steel rocker and bolster bearings is first presented. This theoretical study is used to validate the findings of a high-fidelity finite element model that incorporates contact and friction behavior to accurately capture the performance of older steel bearings under cyclic loads. Given that different bridge configurations result in different levels of vertical (axial) load acting on a bearing, the effect of the vertical load level on the cyclic response of steel bearings is considered. In addition, since steel bridge bearings rely on sliding and rolling to function properly, changes in the friction coefficient at the sliding interface induced by corrosion and debris buildup can influence their mechanical behaviors. Therefore, the influence of the friction coefficient at steel-steel interfaces is also considered as a parameter. The results provide a general understanding of the effect that corrosion can have on the seismic response of steel bearings providing a connection between aging and seismic response that previously has not been thoroughly explored.

2. THEORETICAL ANALYSES OF STEEL BEARINGS

Typical steel rocker and bolster bearings found on bridges constructed in the 1950's and 1960's will be considered. An illustration of the two bearing types is shown in Fig. 2.1 and Fig. 2.3. The theoretical analysis of these bearings will be conducted for displacement in the longitudinal and transverse directions in order to provide an understanding of their expected behavior and a means of verifying the finite element models. A similar approach to that presented by Mander et al. (1996) for other configurations of steel bearings is used to determine the mechanical behavior of these bearings.

2.1. Steel Rocker Bearing

The considered steel rocker bearing has two similar cylindrical surfaces on the top and bottom of the

bearing body as illustrated in Fig. 2.1. The longitudinal behavior of the steel rocker bearing can be determined using rigid body kinematics (Mander et al. 1996). If the top of the rocker bearing is displaced longitudinally by u, then the rocker body will rotate θ. This rotation causes a shift in the points of contact between the bearing surface and the sole plate from E to A and the bearing surface and the masonry plate from F to G as shown in Fig. 2.2(a). Based on this deformed shape, the longitudinal behavior of the rocker bearing can be derived using equilibrium and geometric relationships as given by Eqn. 2.1.

$$H = W \frac{2R - h}{h^2} u \tag{2.1}$$

In Eqn. 2.1, H is the applied longitudinal load required to cause a displacement u; W is the dead load associated with the superstructure; h is the height of the rocker bearing body measured from the two vertices (E and F) at the bearing's top and bottom cylindrical surfaces in its initial configuration; and R is the radius of the top and bottom cylindrical surface. In the derivation of Eqn. 2.1, it is assumed that the rocker bearing remains rigid with no effects associated with local deformation or the presence of the pintles. The vertical load also is assumed to be constant throughout the loading. From Eqn. 2.1, it can be seen that the longitudinal stiffness of the rocker bearing is a function of the applied vertical load, the radius of the cylindrical surfaces, and the height of the rocker body.

The transverse behavior of the rocker bearing can be determined considering equilibrium and stability. Fig. 2.2(b) shows a transversely displaced rocker bearing at the limit state where it begins to tip and become unstable. Considering equilibrium and differentiating, the critical transverse load for this limit state when θ is zero is given by Eqn. 2.2.

$$H_c = W \frac{\omega}{h} \tag{2.2}$$

Eqn. 2.2 shows that the maximum applied lateral load prior to reaching the limit state of tipping is a function of the vertical load, W, the width of the bearing body, ω, and the height of the bearing body, h. In deriving the transverse tipping load, it is assumed that lateral instability occurs prior to shear failure of the anchor bolts or pintles resulting in stability governing the failure mode.
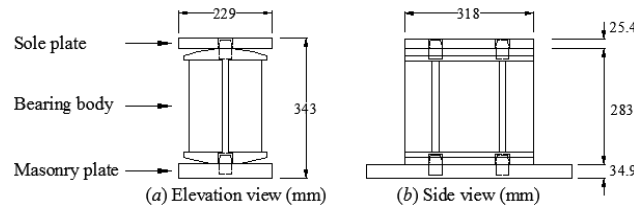

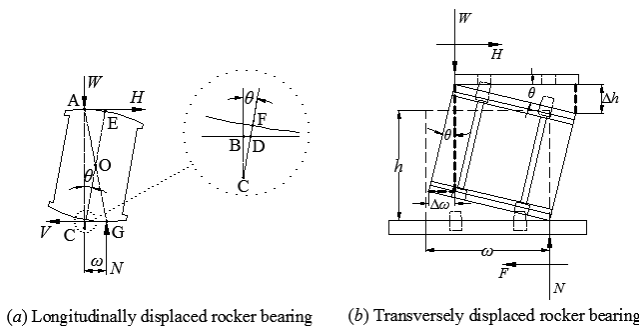**Figure 2.1** Case study rocker (expansion) bearing with typical dimensions

Figure 2.2 Displaced rocker bearing for the theoretical derivations

2.2 Steel Bolster Bearing

Unlike the rocker bearing, the steel bolster bearing only has one cylindrical contact surface at the top of the bearing body as seen in Fig. 2.3. The base of the bearing body is welded directly to the masonry plate which is anchored to the substructure of the bridge providing a rigid connection. A theoretical analysis of the steel bolster bearing considering the loading when the limit state is reached is used to derive the maximum lateral resistance. Two possible failure modes are considered in order to derive the maximum resistance of the bearing in both the longitudinal and transverse loading directions.

The first failure mode consists of rocking of the bolster bearing about the leading edge of the masonry plate along with prying of the anchor bolts embedded in the concrete pedestal. An improved plastic mechanism method, initially proposed by Mander et al. (1996), is adopted for deriving the corresponding lateral load associated with this limit state. The method is improved by utilizing the findings of Kulak et al. (2001) which provides an elliptical relationship for the interaction between the tensile stress and shear stress in the bolt (Eqns. 2.7 and 2.12). The assumed loading at failure is illustrated for both the longitudinal and transverse loading directions in Fig. 2.4. The limit state for the first failure mode is defined by the anchor bolt on the tension side reaching its maximum strength under combined shear and tension and yielding of the bottom of the masonry plate on the leading edge resulting in the formation of a stress block. Based on these assumptions, equations can be derived to estimate the maximum resistance of a bolster bearing displaced in the longitudinal and transverse directions.

For longitudinal displacement:

$$H = 2V_b + \mu \cdot C \tag{2.3}$$

$$C = W + 2T_b \tag{2.4}$$

$$H \cdot h_b = C\left(\frac{\omega_m - a}{2}\right) \tag{2.5}$$

$$C = \sigma_y \cdot a \cdot l_m \tag{2.6}$$

$$\left(\frac{f_t}{F_u}\right)^2 + \left(\frac{f_v}{0.62F_u}\right)^2 = 1 \tag{2.7}$$

For transverse displacement:

$$H = V_b + \mu \cdot C \tag{2.8}$$

$$C = W + T_b \tag{2.9}$$

$$H \cdot h_b + W \cdot l_1 = C\left(l_1 + \frac{l_m - a}{2}\right) \tag{2.10}$$

$$C = \sigma_y \cdot a \cdot \omega_m \tag{2.11}$$

$$\left(\frac{f_t}{F_u}\right)^2 + \left(\frac{f_v}{0.62F_u}\right)^2 = 1 \tag{2.12}$$

H is the applied longitudinal or transverse load; W is the dead load associated with the superstructure; C is the resultant force from the masonry plate bearing on the concrete pedestal; T_b and V_b are the tensile and shear forces acting on the bolt, respectively; σ_y is the yield stress for the masonry plate material; h_b is the height of the bolster bearing body; a is the width of the stress block; ω_m and l_m are the width and length of the masonry plate, respectively; f_t is the tensile stress in the bolt; f_v is the shear stress acting on the shear plane of the bolt; F_u is the tensile strength of the bolt; l_l is the distance between the center lines of the anchor bolt and the bolster bearing body; and μ is the friction coefficient between the masonry plate and concrete pedestal.

The second failure mode is governed by shear failure at the sole plate-bolster bearing body contact interface where the shear capacity is contributed exclusively by the shear resistance of the two pintles and friction between the sole plate and bolster body. The corresponding maximum resistance is given by Equation (2.13) where μ_l is the friction coefficient at the sole plate-bolster body interface, V_p is the shear capacity of a pintle, and n_p is the total number of pintles (2 for the considered bearing configurations).

$$H = \mu_1 W + n_p V_p \qquad (2.13)$$

The maximum lateral resistance of the steel bolster bearings is then determined by taking the minimum value of the calculated resistances for the first and second failure modes. For both modes, the effects of aging and corrosion can play a critical role in reducing the lateral load capacity of the bolster bearing. It should also be noted that the above derivation assumes a perfect bond between the anchor bolts and the concrete pedestal. This assumption is justifiable given proper detailing of reinforcement in the concrete pedestal, but experimental testing is required in order to further evaluate the effects of anchor bolt pullout and concrete pedestal deformation.
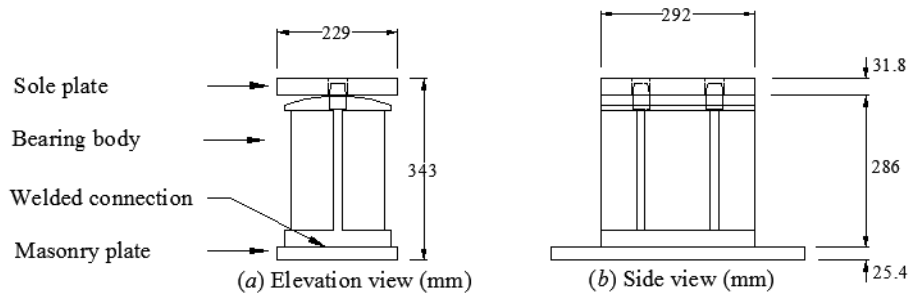

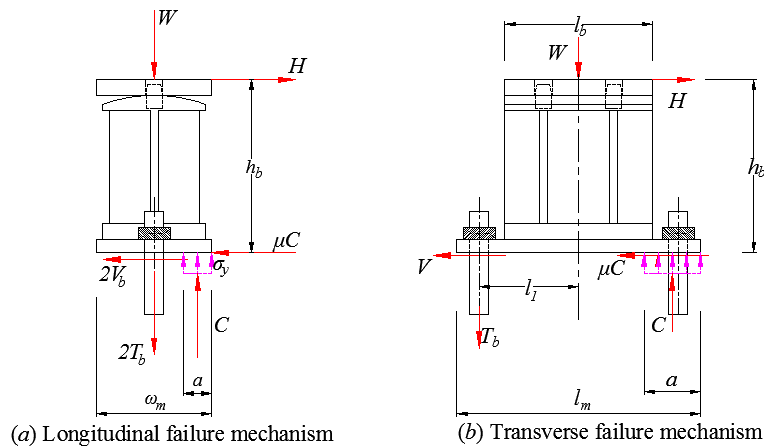**Figure 2.3** Case study bolster (fixed) bearing with typical dimensions

Figure 2.4 Loading for plastic analysis of the bolster bearing

3. FINITE ELEMENT (FE) ANALYSIS OF STEEL BEARINGS

3.1 FE Model Details

The modeling strategy adopted in this study is based on the one described in Fan and McCormick (2011) utilizing the available commercial code, ABAQUS. First-order continuum hexahedral brick elements with incompatible modes are used to model all subcomponents that consider contact and friction, while reduced-integration elements are adopted for all other components of the bearing-pedestal assemblage. At interfaces where two subcomponents interact through contact and friction, such as the bearing body-sole plate interface or bearing body-masonry plate interface, contact pairs are defined between the surfaces in contact with hard contact assumed for behavior normal to the surfaces and Coulomb friction assumed for behavior tangential to the surfaces. A finite sliding formulation that allows for arbitrary sliding, rolling, and separation of the surfaces in contact is adopted for tracking contact while penalty methods are chosen to enforce both the normal and tangential constraints (DS-Simulia 2008). The typical material used in fabricating older steel bearings is mild carbon steel with a minimum required yield strength of 248 MPa. A bilinear material model considering elastic-plastic behavior with strain hardening is adopted for the entire bearing assemblage. Since the steel bearings are the focus of this study, an elastic material model is assigned to the concrete pedestal while the loading beam is assumed rigid. The bearing dimensions are based on those found installed in a typical four-span continuously supported steel girder bridge in the U.S. state of Illinois as shown in Figs. 2.1 and 2.3.

3.2 FE Results for the Steel Rocker Bearing

3.2.1 Longitudinal behavior

Fig. 3.1(a) shows the cyclic response of the steel rocker bearing under multiple cycles of longitudinal displacement reversals with increasing magnitudes of 10.2 mm, 20.3 mm, 30.5 mm, 40.6 mm, and 50.8 mm. A vertical load of 205 kN is applied to the bearing which is typical of an interior bearing of a four-span continuously supported steel girder bridge. A friction coefficient of 0.2 is assumed for the contact interfaces. In general, the response of the rocker bearing is linear with some minor deviations throughout the loading. No degradation in stiffness occurs as the number of loading cycles increases and an identical cyclic response is observed for each loading cycle suggesting a very consistent performance during an earthquake. The findings also closely match the theoretical predication obtained from Eqn. 2.1 with only a minor difference during initial loading where the finite element model shows a much stiffer behavior. However, this behavior is observed over a very small deformation range and is largely associated with the bearing returning to a vertical configuration causing an alignment of the vertical loads. The similarity between the finite element model and theoretical prediction suggests the accuracy of the modelling technique. It should also be noted that 50.8 mm is a significant displacement for a typical steel bearing even under earthquake loads.

Since cycling effects are negligible, the effect of the friction coefficient and vertical load is considered using a single large magnitude cycle. It is observed that the friction coefficient at the steel-steel contact interfaces has little influence on the longitudinal behavior of the rocker bearing. For the three considered friction coefficient values (0.2, 0.3, and 0.4), the cyclic response of the rocker bearing demonstrates essentially the same behavior with an identical secant stiffness of 0.86 kN/mm. This observation is largely due to the fact that the longitudinal behavior of the rocker bearing is governed by rolling friction rather than sliding friction. This is consistent with the theoretical result where the longitudinal stiffness of the rocker bearing is only a function of vertical load, bearing body height, and radius of the cylindrical surfaces. Fig. 3.1(b) shows that the cyclic response for the steel rocker bearing in the longitudinal direction is proportional to the applied vertical load level. For increasing vertical load levels, the secant stiffness of the bearing increased. Secant stiffness values of 0.44 kN/mm, 0.65 kN/mm, 0.86 kN/mm are measured for the vertical loads of 102 kN, 154 kN, and 205 kN, respectively. This parametric study confirms that the longitudinal stiffness of a rocker bearing is proportional to the vertical load acting on it.
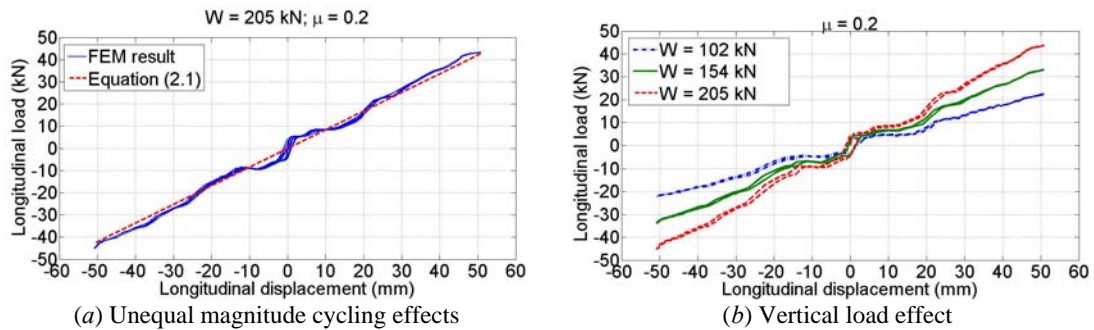
(a) Unequal magnitude cycling effects   (b) Vertical load effect

Figure 3.1 Finite element results for the longitudinal behavior of a steel rocker bearing considering: (a) cyclic loading and cycle magnitude effects and (b) vertical load effects

3.2.2 Transverse behavior

Fig. 3.2(a) presents the response of a steel rocker bearing under transverse displacement reversal with increasing cycle magnitudes of 1.59 mm, 3.18 mm, 3.81 mm, and 5.08 mm. The relatively small maximum displacement is due to the fact that steel bearings are not designed to undergo transverse displacement and thus small displacements are capable of triggering expected failure modes. The 5.08 mm displacement cycle causes the bearing behavior to reach a plateau suggesting inability to resist further displacement. The overall cyclic response of the rocker bearing under progressively increasing displacement reversals shows a predominant sliding behavior within a displacement range of ±3.0 mm and a rapid increase in resistance beyond this displacement range. This sliding is attributed to the gap between the pintles and the holes in which they sit at the top and bottom of the bearing assembly. Once this gap is exhausted, the stiffness in the transverse direction increases as the pintles engage. At even larger displacements, the stiffness of the rocker bearing gradually softens due to plastic deformation of the pintle and the possible onset of rocking. In general, the overall hysteretic response of the bearing exhibits good symmetry with very little degradation due to cycling.

Two sets of parametric studies are conducted to examine the effect of the friction coefficient and the vertical load on the transverse cyclic behavior of the rocker bearing. Since cycling effects are found to be negligible, the rocker bearing is subjected to one full cycle of displacement reversal with a magnitude of 3.18 mm. This transverse displacement level allows the behavior to be considered just up to reaching the point of failure. Fig. 3.2(b) shows that the transverse sliding resistance of the rocker bearing is dependent on the friction coefficient. For this study, the bearing model is subjected to a constant vertical load of 205 kN and considers three friction coefficients of 0.2, 0.3, and 0.4. The results show that the sliding resistance corresponding to the sliding plateaus is the product of the constant vertical load and the varying friction coefficient at the steel-steel contact interfaces with sliding occurring at transverse loads of 44 kN, 66 kN, and 88 kN for the friction coefficients of 0.2, 0.3, and 0.4, respectively. A similar vertical load study as was conducted for longitudinal loading is considered for the bearing under transverse loading with the magnitude of the cycle being ±3.18 mm. The response is very similar to that found when varying the friction coefficient causing the sliding plateaus and hysteresis curves to shift upward due to the higher friction forces associated with the larger normal loads acting at the contact interfaces. The conclusion drawn from the two sets of parametric studies is that the transverse behavior of the rocker bearing is dependent on Coulomb friction in the small displacement range prior to instability or pintle engagement and yielding.

3.2.3 Comparison between finite element and theoretical results

The theoretical load-deformation relationship for the rocker bearing, obtained using Eqn. 2.1 is also included in Fig. 3.1(a). A satisfactory agreement is seen between the numerical and the theoretical results confirming the effectiveness and accuracy of the finite element models. For the transverse behavior of the rocker bearing, the maximum resistances derived from Eqn. 2.2 and from the finite element analyses considering various friction coefficients and vertical loads are very similar where the finite element results slightly under predict the maximum resistance compared to the theoretical equation. This difference is probably associated with the fact that the bearing is assumed rigid in the

theoretical deduction. The finite element analysis and theoretical results both show that the friction coefficient has little effect on the ultimate resistance of the rocker bearings under longitudinal loading. In the case where the friction coefficient is maintained constant, vertical load shows a significant influence on the ultimate resistance of the bearings for all loading cases. The results suggest that effects of aging and corrosion on the friction coefficient will only minimally affect the behavior of the steel rocker bearing under seismic loads. However, other consequences of aging and corrosion such as geometry changes can still be significant and need further exploration.
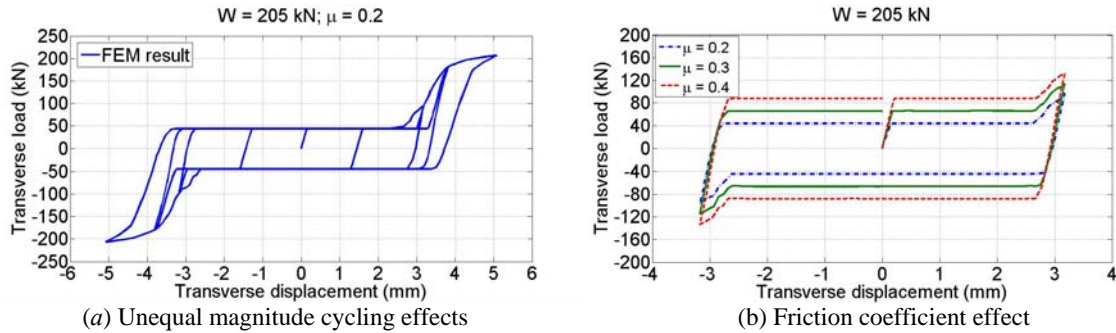

(*a*) Unequal magnitude cycling effects   (b) Friction coefficient effect

Figure 3.2 Finite element results for the transverse behavior of a steel rocker bearing considering: (a) cyclic loading and cycle magnitude effects and (b) effects of varying the friction coefficient at the steel-steel interfaces

3.3 FE Results for the Steel Bolster Bearing

3.3.1 Longitudinal behavior
Fig. 3.3(a) presents the cyclic response of the bolster bearing under displacement loading cycles with progressively increasing magnitudes of 1.6 mm, 3.2 mm, 6.4 mm, 9.5 mm, and 12.7 mm. The response of the bolster bearing under the 1.6 mm displacement cycle, which is less than the gap between the pintle and edge of the hole in the sole-plate within which it rests, is quasi-rectangular suggesting that the behavior is dominated by sliding. This plateau elongates with subsequent larger loading cycles due to plastic deformation of the pintles. The maximum resistance with each loading cycle also gradually increases with the increasing displacement level. Further, a slight degradation in stiffness of the force-deformation response is observed during the negative portion of cycling. The secant stiffness associate with the negative cycles to 6.4 mm, 9.5 mm. and 12.7 mm is 45 kN/mm, 35 kN/mm, 27 kN/mm. The findings suggest that displacement magnitude has a significant effect on the longitudinal behavior of the bolster bearing, while cycling effects are more limited particularly at smaller displacements.
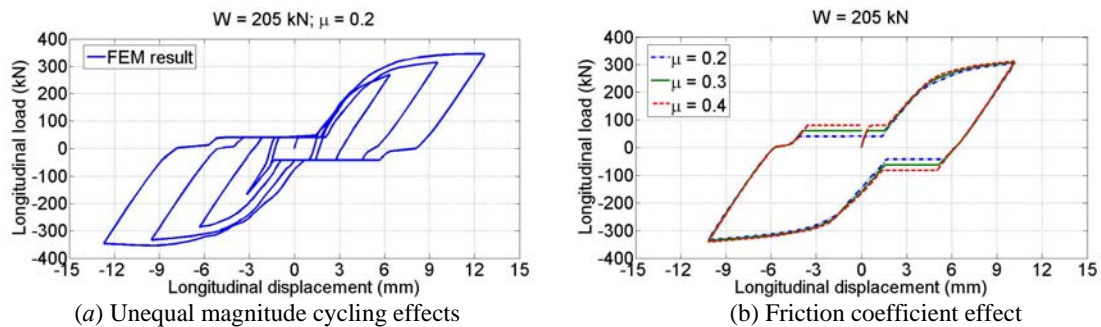

(*a*) Unequal magnitude cycling effects   (b) Friction coefficient effect

Figure 3.3 Finite element results for the longitudinal behavior of a steel bolster bearing considering: (a) cyclic loading and cycle magnitude effects and (b) effects of varying the friction coefficient at the steel-steel interfaces

As reflected in Fig. 3.3(b), the most salient effect of the friction coefficient on the longitudinal behavior of the bolster bearing is that the magnitude of resistance corresponding to the sliding plateau is shifted upward as the friction coefficient increases. With an applied vertical load of 205 kN, the longitudinal force at which the sliding plateau occurs is 40 kN, 60 kN, and 81 kN for a friction

coefficient at the steel-steel interface of 0.2, 0.3, and 0.4. A similar trend is observed for the case where the friction coefficient is taken as constant, 0.2, and the vertical load is varied. For vertical loads of 102 kN, 154 kN, and 205 kN, the longitudinal force plateau at small displacements is measured at 20 kN, 30 kN, and 40 kN, respectively. These results suggest that the longitudinal behavior of the bolster bearing is highly dependent on the applied vertical load and friction coefficient. As a result, aging and corrosion can have a significant effect on the bearing performance under seismic load and the overall performance of the bridge system. The remainder of the hysteretic behavior is not significantly affected by varying the friction coefficient or vertical load.

3.3.2 Transverse behavior

Fig. 3.4(a) shows the results of the cyclic response of the steel bolster bearing under progressively increasing transverse loading cycles with magnitudes of 1.6 mm, 3.2 mm, 4.8 mm, and 6.4 mm. The results suggests a very similar behavior to that observed for the bolster bearing under longitudinal loading where at small displacements the behavior is dominated by sliding and friction and at larger displacements by the plastic deformation of the pintles. An elongation of the sliding plateau is observed as the loading displacement increases. The magnitude of sliding force remains constant throughout cycling and is equal to the product (41 kN) of the applied vertical load (205 kN) and the friction coefficient (0.2). At intermediate displacements, engagement of the pintles also will transfer large shear forces to the bolster bearing body and lead to prying of the bolster bearing on the pedestal causing the observed increase in stiffness until plastic deformation of the pintles occurs. The findings suggest that displacement magnitude has a significant effect on the transverse behavior of the bolster bearing, while cycling effects are more limited.

The influence of the friction coefficient at the steel-steel interface (Fig. 3.4(b)) and the vertical load level on the cyclic response of the bolster bearing in the transverse direction is examined using one full loading cycle under a relatively high displacement magnitude, 5 mm. The transverse load corresponding to the sliding plateau increases from 40 kN to 81 kN with an increase in the friction coefficient at the steel-steel interface from 0.2 to 0.4. Overall, the friction coefficient causes an outward shift of the whole hysteresis curve. A similar observation is also made for the influence of vertical load level. From these two parametric studies, it is further confirmed that sliding with Coulomb friction dominates the deformation mode of the bolster bearing under small transverse displacements. As a result, corrosion can have a significant effect on the bearing performance under seismic load.
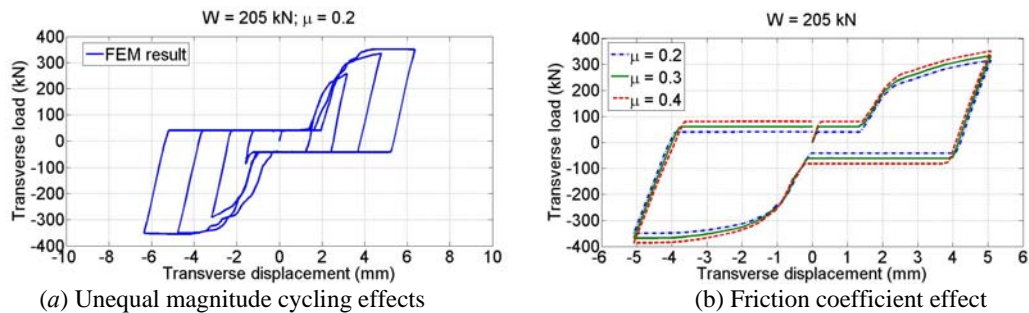

(a) Unequal magnitude cycling effects
(b) Friction coefficient effect

Figure 3.4 Finite element results for the transverse behavior of a steel bolster bearing considering: (a) cyclic loading and cycle magnitude effects and (b) effects of varying the friction coefficient at the steel-steel interfaces

3.3.3 Comparison between FEM and theoretical results

The theoretical maximum resistance obtained for steel bolster bearings using a plastic mechanism analysis, as governed by Eqns. 2.3-2.13, and that obtained from the finite element analyses is compiled in Table 3.1 for both the longitudinal and transverse loading directions. For the longitudinal loading, the difference in the maximum resistance obtained through the theoretical analyses and finite element analyses is on average 6% suggesting a good agreement between the two approaches and the accuracy of the finite element model. For the transverse maximum resistance prediction, the theoretical

prediction matches closely with the finite element model results at low friction coefficients and all vertical load levels again suggesting the accuracy of the finite element model. In all cases, the finite element model tended to predict lower values compared to the theoretical formulation. The results suggest that effects of aging and corrosion on the friction coefficient will have a significant impact on the behavior of the steel bolster bearings under seismic loads.

Table 3.1 Maximum resistance for the steel bolster bearings

Bearing type/Loading direction	Term	Friction coefficient			Vertical load (kN)		
		0.2	*0.3*	*0.4*	*102*	*154*	*205*
Bolster/Longitudinal	FEM	334	334	334	315	325	334
	Theoretical	359	367	364	329	344	359
Bolster/Transverse	FEM	340	359	379	320	330	338
	Theoretical	349	387	430	326	338	349

5. CONCLUSIONS

A theoretical and finite element study of the longitudinal and transverse behavior of steel rocker and bolster bridge bearings is undertaken. The possible influence of aging and corrosion on the seismic response of the bearings is explored through varying of the friction coefficient and vertical load levels. The results provide a finite element model that can accurately capture the cyclic behavior of steel bearings and suggest that the performance of steel bolster bearings is significantly affected by corrosion. Other work is on-going to explore other aging effects, such as changes in geometry due to corrosion, and how the bearing performance affects the seismic response of a full bridge system.

REFERENCES

Barker, M.G. and Hartnagel, B.A. (1998). Longitudinal restraint response of existing bridge bearings. *Transportation Research Record* **Issue 1624**,28-35.

Brinkerhoff, P. (1993). Bridge Inspection and Rehabilitation: A Practical Guide, Wiley and Sons Inc., New York, NY.

Dicleli, M. and Bruneau, M. (1995). Seismic performance of multispan simply supported slab-on-girder steel highway bridges. *Engineering Structures* **17:1**,4-14.

DS-Simulia (2008). ABAQUS version 6.8-1 Documentation, Providence, RI.

Fan, X. and McCormick, J. (2011). Finite element analysis of the cyclic behaviour of corroded bridge bearings. *The 2011 World Congress on Advances in Structural Engineering and Mechanics*, Seoul, Korea.

Kayser, J.R., and Nowak, A.S. (1989). Capacity loss due to corrosion in steel girder bridges. *Journal of Structural Engineering* **115:3**,1525-1537.

Kulak, G.L., Fisher, J.W., and Struik, J.H. (2001). Guide to Design Criteria for Bolted and Riveted Joints, 2nd Edition, American Institute of Steel Construction Inc., Chicago, IL.

Mander, J.B., Kim, D-K., Chen, S.S., and Premus, G.J. (1996). Response of Steel Bridge Bearings to Reversed Cyclic Loading, Technical Report NCEER-96-0014, National Center for Earthquake Engineering Research.

Nielson, B. and DesRoches, R. (2007). Seismic fragility curves for typical highway bridge classes in the Central and Southeastern United States. *Earthquake Spectra*, **23:3**, 615-633.

Padgett, J.E. and DesRoches, R. (2008). Three-dimensional nonlinear seismic performance evaluation of retrofit measures for typical steel girder bridges. *Engineering Structures* **30:7**, 1869-1878.

Pan, Y., Agrawal, A.K., Ghosn, M., and Alampalli, S. (2010). Seismic fragility of multispan simply supported steel highway bridges in New York State. I: Bridge modeling, parametric analysis, and retrofit design. *Journal of Bridge Engineering* **15:5**,448-461.

Shinozuka, M., Feng, M.Q., Kim, H-K., and Kim, S-H. (2000). Nonlinear static procedure for fragility curve development. *Journal of Engineering Mechanics* **126:12**, 1287-1296.

Splitstone, D.E., Stonecheck, S.A., Dodson, R.L., and Fuller, J.A. (2010). Birmingham bridge emergency repairs: Micropile foundation retrofit. *GeoFlorida 2010: Advances in Analysis, Modelling, & Design*. FL.

Unjoh, S., Sugiyama, T., Sakai, J. and Okada, T. (2008). Damage of Bridge Structures during Recent Earthquakes and the Effectiveness of Seismic Retrofit. *Proc. of the 40th Joint Meeting of UJNR Wind and Seismic Effects*. 1-13.